Phytochemistry xxx (2016) 1–9

Contents lists available at ScienceDirect

Phytochemistry

journal homepage: www.elsevier.com/locate/phytochem

Amides and neolignans from the aerial parts of *Piper bonii*

Duo-Duo Ding [a, 1], Yue-Hu Wang [a, 1], Ya-Hui Chen [b], Ren-Qiang Mei [a], Jun Yang [a], Ji-Feng Luo [a], Yan Li [c], Chun-Lin Long [a, d, *], Yi Kong [b, **]

[a] Key Laboratory of Economic Plants and Biotechnology, Yunnan Key Laboratory for Wild Plant Resources, Kunming Institute of Botany, Chinese Academy of Sciences, Kunming 650201, People's Republic of China
[b] School of Life Science & Technology, China Pharmaceutical University, Nanjing 210009, People's Republic of China
[c] State Key Laboratory of Phytochemistry and Plant Resources in West China, Kunming Institute of Botany, Chinese Academy of Sciences, Kunming 650201, People's Republic of China
[d] College of Life and Environmental Sciences, Minzu University of China, Beijing 100081, People's Republic of China

ARTICLE INFO

Article history:
Received 6 February 2016
Received in revised form
28 June 2016
Accepted 13 July 2016
Available online xxx

Keywords:
Piper bonii
Piperaceae
Amides
Neolignans
Antiplatelet

ABSTRACT

Six amides, piperbonamides A–F, three neolignans piperbonins A–C, and 11 known compounds were isolated from the aerial parts of *Piper bonii* (Piperaceae). The structures of piperbonamides A–F and piperbonins A–C were elucidated based on the analysis of 1D and 2D NMR and MS data. Piperbonin A, (+)-*trans*-acuminatin, (+)-*cis*-acuminatin, (+)-kadsurenone, and pipernonaline showed weak activity against platelet aggregation with IC_{50} values of 118.2, 108.5, 90.02, 107.3, and 116.3 μM, respectively, as compared with the positive control, tirofiban, with an IC_{50} value of 5.24 μM. Piperbonamides A–F were inactive against five tumor cell lines at concentrations up to 40 μM.

1. Introduction

Antiplatelet therapy is a milestone in the primary and secondary prevention of atherothrombotic diseases. Abundant recent data support that traditional Chinese herbs and their active constituents may be a good alternative and complementary choice for new antiplatelet drugs (Chen et al., 2015; Zhang et al., 2015). For example, ginkgolide B from the leaf of *Ginkgo biloba* L. significantly inhibited rabbit platelet aggregation induced by platelet-activating factor (PAF) with an IC_{50} value of 0.128 μM (Hu et al., 2000).

The genus *Piper* (Piperaceae) is a medicinally important group of plants consisting of approximately 2000 species worldwide. There are approximately 60 species distributed in the tropical areas of the People's Republic of China, of which approximately 30 species have been used as traditional Chinese medicine (Tseng et al., 1999; Wang et al., 2014b). Some *Piper* species, including *Piper betle* L., *Piper boehmeriifolium* (Miq.) Wall. ex C. DC., *Piper hongkongense* C. DC., *Piper kadsura* (Choisy) Ohwi, *Piper laetispicum* C. DC., *Piper macropodum* C. DC., *Piper mutabile* C. DC., *Piper puberulilimbum* C. DC, *Piper sarmentosum* Roxb., *Piper wallichii* (Miq.) Hand.-Mazz., and *Piper yunnanense* Tseng, are used for promoting blood circulation ("Huoxue" in Chinese) (Editorial Board of "Zhonghua Bencao", 1999). Traditional Chinese medicines with functions of "Huoxue" or "Huayu" (removing blood stasis) are claimed to be useful in antiplatelet therapies and in the treatment of thrombotic diseases (Chen et al., 2015; Liu et al., 2012). Thus, from herbs used to promote blood circulation and/or remove blood stasis, active compounds against platelet aggregation might be obtained. For example, salvianolic acids A and B from *Salvia miltiorrhiza* Bunge (Huang et al., 2010; Liu et al., 2014), the dihydrochalcone loureirin A from *Dracaena cochinchinensis* (Lour.) SC Chen (Hao et al., 2015; Xin et al., 2011), and the alkaloid tetramethylpyrazine from *Ligusticum striatum* DC. were reported to possess potent antiplatelet activity (Sheu et al., 1997; Wang et al., 2013).

Amides, phenylpropanoids, lignans, and neolignans are the major constituents of *Piper* plants (Kato and Furlan, 2007; Parmar et al., 1997; Scott et al., 2008). These compounds showed various biological activities, including antiplatelet effects (Chen et al., 2014,

* Corresponding author.
** Corresponding author.
E-mail addresses: long@mail.kib.ac.cn (C.-L. Long), yikong668@163.com (Y. Kong).
[1] These authors contributed equally to this work.

http://dx.doi.org/10.1016/j.phytochem.2016.07.004
0031-9422/

2013, 2007; Fontenele et al., 2009; Iwashita et al., 2007; Li et al., 2007; Park et al., 2007; Shi et al., 2015). *Piper bonii* C. DC. is a climbing liana distributed mainly in the Chinese provinces of Guangxi, Hainan, and Yunnan, and in northern Vietnam (Tseng et al., 1999). However, the chemical constituents of *P. bonii* are unknown. In continuing efforts to search for bioactive constituents from *Piper* plants (Liu et al., 2015; Tang et al., 2011; Yang et al., 2013a, 2013b), the results of the analysis of compounds from the aerial parts of *P. bonii*, and the bioactivity of several of these compounds, are reported.

2. Results and discussion

Chromatographic separation of the MeOH soluble part of the aerial parts of *P. bonii* led to isolation of 20 compounds, including nine new compounds (**1**–**9**, Fig. 1) and 11 known compounds (**10**–**20**).

The molecular formula of piperbonamide A (**1**), $C_{27}H_{33}NO_3$, was determined by ^{13}C NMR data and an HRESIMS ion at *m/z* 442.2352 $[M+Na]^+$ (calcd for $C_{27}H_{33}NNaO_3$, 442.2353), and required 12 indices of hydrogen deficiency. Its IR spectrum showed absorption peaks for a secondary amide at 3396 and 1657 cm^{-1}. Absorptions at 1627, 1610, 1596, 1532, 1514, and 1449 cm^{-1} suggested the presence of phenyl rings and double bonds. The ^1H NMR data (Table 1) indicated two *p*-disubstituted phenyl rings [δ_H 6.96 (2H, br d, $J = 8.6$ Hz, H-2′,6′) and 6.68 (2H, br d, $J = 8.6$ Hz, H-3′,5′); 7.03 (2H, d, $J = 8.6$ Hz, H-2″,6″) and 6.70 (2H, d, $J = 8.6$ Hz, H-3″,5″] and three double bonds, including two *E* double bonds ($J_{2,3} = 15.1$ Hz and $J_{4,5} = 15.1$ Hz). The ^{13}C NMR data (Table 1) exhibited eight methylenes, 14 methines, two sp^2 quaternary carbons [δ_C 133.1 (C-1′) and 131.3 C-1″)], two oxygenated sp^2 tertiary carbons [δ_C 156.9 (C-4″) and 156.5 (C-4′)], and an amide carbonyl carbon (δ_C 169.1). Comparison of its NMR data with those of known compounds from other *Piper* plants species (Tang et al., 2011; Yang et al., 2013a) suggested that the compound might be an arylalkenylacyl amide.

^1H–^1H COSY correlations (Fig. 2) exhibited three partial structures comprising C-2 to C-11, C-12 to C-13, and C-7″ to C-8″. On the basis of the HMBC correlations (Fig. 2) from H-3 to C-1, H-12 to C-1′, H_2-13 to C-11, C-2′ and C-6′, the acyl fragment was confirmed to be a 13-(4-hydroxyphenyl)-2,4,11-tridecatrienacyl moiety. In addition, the HMBC correlation of H_2-8″ to C-1″, H_2-7″ to C-2″ and C-6″, confirmed the amido fragment as a 2-(4-hydroxyphenyl)ethylamino moiety. The *E* geometry of the C-11–C-12 double bond was established by comparison of the ^{13}C NMR chemical shifts of the allylic carbons [δ_C 39.2 (C-13) and 33.4 (C-10)] with those in the *Z* analogue, sarmentosumol A [δ_C 32.5 (C-1′) and 27.2 (C-4′)] (Yang et al., 2013b), and the *E* analogue, marginatine [δ_C 39.0 (C-1′) and 32.7 (C-4′)] (Santos et al., 1998). Therefore, the structure of compound **1** (piperbonamide A) was defined as (2*E*,4*E*,11*E*)-*N*-[(4-hydroxyphenyl)ethyl]-13-(4-hydroxyphenyl)-2,4,11-tridecatrienamide.

The molecular formula of piperbonamide B (**2**), $C_{27}H_{35}NO_3$, was determined by analysis of ^{13}C NMR and HRESIMS data. The NMR data of **2** (Table 1) resembled those of **1** and showed that the signals for a double bond in **1** were replaced by the signals for two methylene groups in **2**. Based on its 2D NMR correlations (Fig. S1, Supplementary data), the two double bonds of **2** were located at C-2 and C-11, respectively. The *E* geometry of the double bonds was determined by the *J* values (both $J_{2,3} = 15.5$ Hz) of the olefinic protons and the ^{13}C NMR chemical shifts of the allylic carbons [δ_C 39.2 (C-13) and 33.5 (C-10)]. Thus, compound **2** (piperbonamide B) was identified as (2*E*,11*E*)-*N*-[(4-hydroxyphenyl)ethyl]-13-(4-hydroxyphenyl)-2,11-tridecadienamide.

Piperbonamide C (**3**) gave a molecular formula of $C_{29}H_{37}NO_3$, as deduced by ^{13}C NMR and HRESIMS data. A comparison of the NMR data of **3** with those of **1** (Table 1) indicated that there were signals for two additional methylene groups in **3**. On the basis of 2D NMR correlations (Fig. S1, Supplementary data), compound **3** (piperbonamide C) was identified as (2*E*,4*E*,13*E*)-*N*-[(4-hydroxyphenyl) ethyl]-15-(4-hydroxyphenyl)-2,4,13- pentadecatrienamide, of which three double bonds were determined to be in an *E*-configuration this being based on coupling constants ($J_{2,3} = 15.1$ Hz and $J_{4,5} = 15.1$ Hz) of the olefinic protons, as well as the ^{13}C NMR chemical shifts of the allylic carbons [δ_C 39.2 (C-13) and 33.5 (C-10)].

The molecular formula of piperbonamide D (**4**), $C_{26}H_{31}NO_4$, was determined by ^{13}C NMR data and an HRESIMS ion at *m/z* 444.2144 $[M+Na]^+$ (calcd for $C_{26}H_{31}NNaO_4$, 444.2145), indicating 12 degrees of unsaturation. The ^1H NMR data (Table 2) indicated one 1,2,4-trisubstituted phenyl ring [δ_H 6.89 (br s, H-2′), 6.75 (br d, $J = 7.9$ Hz, H-6′) and 6.73 (d, $J = 7.9$ Hz, H-5′)], one *p*-disubstituted phenyl ring [δ_H 7.04 (2H, d, $J = 8.3$ Hz, H-2″,6″) and 6.78 (2H, d, $J = 8.3$ Hz, H-3″,5″)], two *E* double bonds [δ_H 6.83 (dt, $J = 15.2$, 6.9 Hz, H-3) and 5.68 (d, $J = 15.2$ Hz, H-2); 6.27 (d, $J = 15.8$ Hz, H-11) and 6.03 (dt, $J = 15.8$, 7.1 Hz, H-10)], and one methylenedioxy group [δ_H 5.93 (2H, s)]. By comparing its NMR data with those of compounds **1**–**3**, compound **4** should also be an arylalkenylacyl amide.

The ^1H–^1H COSY correlations (Fig. S1, Supplementary data) exhibited two partial structures comprising C-2 to C-11 and C-7″ to C-8″. Based on the HMBC correlations (Fig. S1, Supplementary data) from H-3 to C-1, H-10 to C-1′, H-11 to C-2′ and C-6′, H-2′ to C-4′, H-5′ to C-3′, and –OCH_2O- to C-3′ and C-4′, the acyl fragment was confirmed as a (2*E*,10*E*)-11-(3,4-methylenedioxyphenyl)-2,10-undecadienacyl moiety. In addition, the HMBC correlations of H_2-

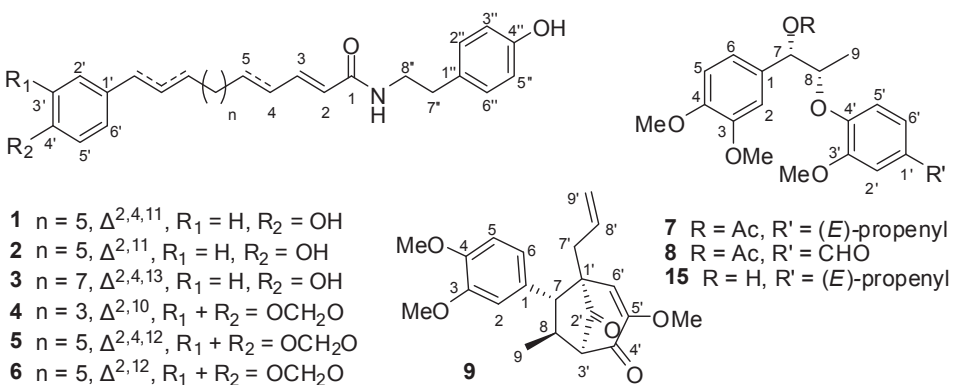

Fig. 1. Structures of compounds **1**–**9** and **15**.

Please cite this article in press as: Ding, D.-D., et al., Amides and neolignans from the aerial parts of *Piper bonii*, Phytochemistry (2016), http://dx.doi.org/10.1016/j.phytochem.2016.07.004

Table 1
^{1}H (600 MHz) and ^{13}C NMR (100 MHz) data of piperbonamides A–C (**1**–**3**) in methanol-d_4.

No.	Piperbonamide A (**1**)		Piperbonamide B (**2**)		Piperbonamide C (**3**)	
	δ_H (J in Hz)	δ_C	δ_H (J in Hz)	δ_C	δ_H (J in Hz)	δ_C
1		169.1		168.8		169.1
2	5.87 d (15.1)	123.0	5.87 br d (15.5)	124.7	5.87 d (15.1)	122.9
3	7.10 dd (15.1, 10.8)	142.2	6.75 dt (15.5, 7.1)	145.7	7.11 dd (15.1, 10.7)	142.2
4	6.17 dd (15.1, 10.8)	129.8	2.18 q like (7.1)	33.0	6.18 dd (15.1, 10.7)	129.8
5	6.08 dt (15.1, 7.0)	144.1	1.44 m	29.4	6.09 dt (15.1, 7.1)	144.2
6	2.16 q like (7.0)	33.9	1.31 m	30.3[a]	2.16 q like (7.1)	33.9
7	1.43 m	29.7	1.31 m	30.2[a]	1.43 m	30.0
8	1.33 m	29.8	1.31 m	30.1[a]	1.31 m	30.3[b]
9	1.39 m	30.4	1.38 m	30.6	1.31 m	30.3[b]
10	2.02 q like (6.8)	33.4	2.02 q like (6.8)	33.5	1.31 m	30.1[b]
11	5.45 m	132.1	5.44 m	132.2	1.38, m	30.6
12	5.52 m	131.2	5.51 m	131.1	2.02 m	33.5
13	3.20 d (6.5)	39.2	3.20 d (6.4)	39.2	5.45 m	132.2
14					5.51 m	131.1
15					3.20 d (6.4)	39.2
1′		133.1		133.1		133.1
2′,6′	6.96 br d (8.6)	130.4	6.96 d (8.4)	130.3	6.96 d (8.5)	130.3
3′,5′	6.68 br d (8.6)	116.1	6.67 d (8.4)	116.0	6.68 d (8.5)	116.0
4′		156.5		156.5		156.5
1″		131.3		131.3		131.3
2″,6″	7.03 d (8.6)	130.7	7.02 d (8.4)	130.7	7.02 d (8.4)	130.7
3″,5″	6.70 d (8.6)	116.2	6.70 d (8.4)	116.2	6.70 d (8.4)	116.2
4″		156.9		156.9		156.9
7″	2.71 t (7.3)	35.8	2.71 t (7.5)	35.7	2.71 t (7.4)	35.8
8″	3.41 t (7.3)	42.5	3.39 t (7.5)	42.4	3.40 t (7.4)	42.6

[a,b]Data under the same entry are interchangeable.

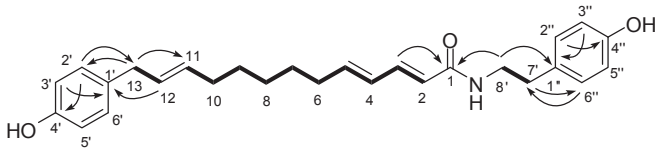

Fig. 2. Selected $^{1}H-^{1}H$ COSY (bold) and HMBC (arrows) correlations of **1**.

8″ to C-1″, and H_2-7″ to C-2″ and C-6″ (Fig. S1, Supplementary data) confirmed that the amido fragment was a 2-(4-hydroxyphenyl) ethylamino moiety. From the HMBC correlations of H_2-8″/C-1, NH/C-1, and NH/C-8″, the two fragments may be connected via an amide bond. Accordingly, the structure of **4** (piperbonamide D) was defined as (2*E*,10*E*)-*N*-[(4-hydroxyphenyl)ethyl]-11-(3,4-methylenedioxyphenyl)-2,10- undecadienamide.

The molecular formula of piperbonamide E (**5**), $C_{28}H_{33}NO_4$, was determined by ^{13}C NMR and HRESIMS data. The NMR data of **5** (Table 2) were similar to those of **4**. However, the NMR signals of **5** showed the presence of three double bonds in **5**. On the basis of the $^{1}H-^{1}H$ COSY and HMBC spectra of **5** (Fig. S1, Supplementary data), the structure of the amide was defined as *N*-[(4-hydroxyphenyl) ethyl]-13-(3,4-methylenedioxyphenyl)-2,4,12-tridecatrienamide. The *E*-geometry of the three double bonds in **5** was defined by the J values ($J_{2,3} = 15.0$ Hz, $J_{4,5} = 15.3$ Hz, and $J_{12,13} = 15.8$ Hz). Hence, compound **5** (piperbonamide E) is (2*E*,4*E*,12*E*)-*N*-[(4-hydroxyphenyl)ethyl]-13-(3,4-methylenedioxyphenyl)-2,4,12-tridecatrienamide.

Piperbonamide F (**6**) had the molecular formula $C_{28}H_{35}NO_4$ based on ^{13}C NMR and HRESIMS analysis. A comparison of the NMR data of **6** (Table 2) with those of **5** indicated that the signals for one double bond in **6** was absent. The remaining two double bonds in **6** were located at C-2 and C-12 from an analysis of its 2D NMR correlations (Fig. S1, Supplementary data). Both double bonds were in an *E*-configuration on the $J_{2,3} = 15.3$ Hz and $J_{12,13} = 15.7$ Hz values. Therefore, compound **6** (piperbonamide F) is (2*E*,12*E*)-*N*-[(4-hydroxyphenyl)ethyl]-13-(3,4-methylenedioxyphenyl)-2,12-tridecadienamide.

Piperbonin A (**7**) had the molecular formula $C_{23}H_{28}O_6$ with 10 degrees of unsaturation based on ^{13}C NMR data and an HRESIMS ion at m/z 423.1781 $[M]^+$ (calcd for $C_{23}H_{28}NaO_6$, 423.1778). Its IR spectrum showed absorption peaks for carbonyl 1737 cm^{-1}, alkenyl (1630 cm^{-1}), and aromatic (1604, 1596, 1512, 1465, and 1453 cm^{-1}) groups. The ^{1}H NMR data (Table 3) showed one *E* propenyl group [δ_H 6.32 (dd, J = 15.7, 1.5 Hz), 6.11 (m) and 1.85 (3H, dd, J = 6.7, 1.5 Hz)], two 1,2,4-trisubstituted phenyl rings [δ_H 6.94 (dd, $J = 8.3$, 1.9 Hz), 6.91 (d, $J = 1.9$ Hz) and 6.82 (d, $J = 8.3$ Hz); δ_H 6.88 (d, $J = 1.9$ Hz), 6.88 (d, $J = 8.3$ Hz) and 6.83 (dd, $J = 8.3$, 1.9 Hz)], three methoxy groups [δ_H 3.87 (3H, s), 3.85 (3H, s) and 3.83 (3H, s)], and two methyl groups [δ_H 1.99 (3H, s) and 1.16 (3H, d, $J = 6.4$ Hz)]. The NMR data of **7** (Table 3) were close to those of a known neolignan (1*R*,2*R*)-2-[2-methoxy-4-(*E*)-prop-1-enyl)phenoxy]-1-(3,4-dimethoxyphenyl)propyl acetate, which was first synthesized and then isolated from *Taxillus theifer* (Hayata) H.S. Kiu (Curti et al., 2006; Lin et al., 2011). However, compound **7** had a positive optical rotation value rather than the negative value for the known neolignan. By 2D NMR correlations of **7** (Fig. 3), its 2D structure was identical to the known compound. The 7,8 relative configuration of **7** was determined as *threo* according to the $J_{7,8}$ value of 7.2 Hz as opposed to 8 and 3 Hz for neolignans with the *threo* and *erythro* configurations, respectively (Braga et al., 1984; Cao et al., 2015; Curti et al., 2006). Compound **7** is the enantiomer of (1*R*,2*R*)-2-[2-methoxy-4-(*E*)-prop-1-enyl)phenoxy]-1-(3,4-dimethoxyphenyl) propyl acetate. Therefore, compound **7** (piperbonin A) is (7*S*,8*S*)-7-acetoxy-3,3′,4-trimethoxy-8,4′-oxyneolign-7′-ene.

Piperbonin B (**8**) had the molecular formula $C_{21}H_{24}O_7$ based on ^{13}C NMR and HREIMS data. Its IR spectrum showed absorption peaks for an ester carbonyl group at 1739 cm^{-1}, an aromatic formyl group at 1684 cm^{-1}, and phenyl rings at 1593, 1508, and 1465 cm^{-1}. The NMR data of **8** (Table 3) were similar to those of **7**, except that signals for the propenyl group were absent and resonances for one formyl group [δ_H 9.85 (s); δ_C 191.0)] were observed in **8**, implying

Please cite this article in press as: Ding, D.-D., et al., Amides and neolignans from the aerial parts of *Piper bonii*, Phytochemistry (2016), http://dx.doi.org/10.1016/j.phytochem.2016.07.004

Table 2
^{1}H (600 MHz) and ^{13}C NMR (100 MHz) NMR data of piperbonamides D–F (**4**–**6**) in $CDCl_3$.

No.	Piperbonamide D (**4**)		Piperbonamide E (**5**)		Piperbonamide F (**6**)	
	δ_H (*J* in Hz)	δ_C	δ_H (*J* in Hz)	δ_C	δ_H (*J* in Hz)	δ_C
1		166.3		166.6		166.3
2	5.68 d (15.2)	123.5	5.67 d (15.0)	121.5	5.68 d (15.3)	123.4
3	6.83 dt (15.2, 6.9)	145.3	7.19 dd (15.0, 9.8)	141.8	6.82 dt (15.3, 6.9)	145.4
4	2.14 m	32.1	6.09 dd (15.3, 9.8)	128.3	2.14 m	32.2
5	1.43 m	28.3	6.06 m	143.7	1.41 m	28.4
6	1.31 m	29.1	2.15 m	33.0	1.28 m	29.5[a]
7	1.31 m	29.1	1.41 m	28.8	1.28 m	29.5[a]
8	1.43 m	29.4	1.31 m	29.1	1.28 m	29.5[a]
9	2.16 m	33.0	1.31 m	29.1	1.28 m	29.3[a]
10	6.03 dt (15.8, 7.1)	129.5	1.43 m	29.5	1.44 m	29.6
11	6.27 d (15.8)	129.5	2.15 m	33.0	2.16, m	33.0
12			6.03 m	129.5	6.04 dt (15.7, 7.0)	129.6
13			6.27 d (15.8)	129.4	6.27 d (15.7)	129.4
1′		132.6		132.6		132.6
2′	6.89 br s	105.5	6.89 d (1.2)	105.5	6.89 d (1.3)	105.5
3′		148.0		148.0		148.0
4′		146.7		146.7		146.8
5′	6.73 d (7.9)	108.4	6.73 d (7.9)	108.4	6.73 d (8.1)	108.4
6′	6.75 br d (7.9)	120.3	6.75 dd (7.9, 1.2)	120.3	6.75 dd (8.1, 1.3)	120.3
1″		130.8		130.8		130.9
2″,6″	7.04 d (8.3)	130.0	7.03 d (8.4)	130.0	7.05 d (8.4)	130.0
3″,5″	6.78 d (8.3)	115.7	6.78 d (8.4)	115.7	6.78 d (8.4)	115.7
4″		154.6		154.7		154.6
7″	2.76 t (6.8)	34.9	2.67 t (6.8)	34.9	2.76 t (6.9)	34.9
8″	3.54 m	40.9	3.55 m	41.1	3.54 m	40.9
OCH_2O	5.93 s	101.0	5.93 s	101.0	5.93 s	101.0
NH	5.44 t (5.5)		5.50 t (5.9)		5.42 t (5.4)	

[a] Data under the same entry are interchangeable.

Table 3
^{1}H and ^{13}C NMR data of piperbonins A–C (**7**–**9**) in $CDCl_3$.

No.	Piperbonin A (**7**)		Piperbonin B (**8**)		Piperbonin C (**9**)	
	δ_H (*J* in Hz)[a]	δ_C[b]	δ_H (*J* in Hz)[c]	δ_C[d]	δ_H (*J* in Hz)[c]	δ_C[d]
1		129.8		129.3		132.8
2	6.91 d (1.9)	110.6	6.91 d (1.9)	110.7	6.51 br s	111.1
3		148.8		149.0		149.0
4		148.9		149.3		148.3
5	6.82 d (8.3)	110.8	6.84 d (8.2)	111.0	6.80 d (8.2)	111.1
6	6.94 dd (8.3, 1.9)	120.0	6.95 dd (8.2, 1.9)	120.2	6.62 br d (8.2)	120.9
7	5.89 d (7.2)	78.2	5.93 d (7.1)	77.8	2.71 d (5.5)	58.0
8	4.55 m	78.1	4.74 m	77.6	2.64 m	38.8
9	1.16 d (6.4)	16.8	1.24 d (6.4)	16.6	1.08 d (7.1)	18.0
1′		132.3		130.6		56.2
2′	6.88 d (1.9)	109.5	7.42 d (1.8)	110.1		203.4
3′		150.5		150.7	3.74 d (7.6)	67.5
4′		147.0		153.6		191.3
5′	6.88 d (8.3)	117.0	7.08 d (8.1)	114.2		153.1
6′	6.83 dd (8.3, 1.9)	118.6	7.44 dd (8.1, 1.8)	126.5	6.28 s	123.0
7′	6.32 dd (15.7, 1.5)	130.5	9.85 s	191.0	2.22 dd (14.8, 7.9)	33.9
					2.05 dd (14.8, 7.0)	
8′	6.11 m	124.2			5.64 m	133.2
9′	1.85 dd (6.7, 1.5)	18.4			5.07 br d (10.0)	119.2
					5.04 br d (17.1)	
3-OMe	3.87 s	55.9	3.89 s	56.0	3.86 s	55.8
4-OMe	3.85 s	55.8	3.88 s	56.0	3.87 s	55.9
3′-OMe	3.83 s	55.8	3.91 s	56.1		
5′-OMe					3.70 s	55.6
OAc		170.0		170.1		
	1.99 s	21.1	2.00 s	21.2		

[a] Measured at 500 MHz.
[b] measured at 125 MHz.
[c] measured at 600 MHz.
[d] measured at 100 MHz.

that it should be a dinorneolignan. On the basis of the 2D NMR correlations (Fig. S1, Supplementary data), the 2D structure of compound **8** was deduced to be 7-acetoxy-3,3′,4-trimethoxy-8′,9′-dinor-8,4′-oxyneolignan-7′-al. Like compound **7**, the relative configuration of **8** was also determined as *threo* ($J_{7,8}$ = 7.1 Hz). The absolute configuration of **8** (piperbonin B) was not determined as

Please cite this article in press as: Ding, D.-D., et al., Amides and neolignans from the aerial parts of *Piper bonii*, Phytochemistry (2016), http://dx.doi.org/10.1016/j.phytochem.2016.07.004

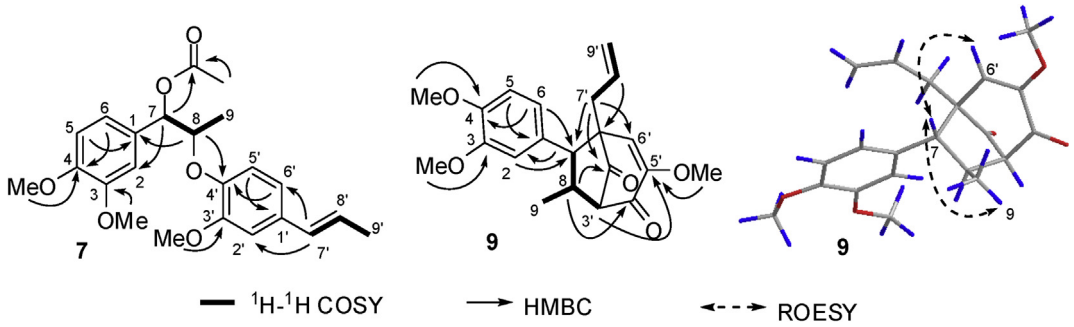

Fig. 3. Key 2D NMR correlations of compounds **7** and **9**.

yet.

The molecular formula $C_{21}H_{24}O_5$ assigned to compound **9** was determined by ^{13}C NMR data and an HRESIMS ion at *m/z* 379.1520 $[M+Na]^+$ (calcd for $C_{21}H_{24}NaO_5$, 379.1516) with 10 degrees of unsaturation. The IR spectrum showed absorption bands for carbonyl (1759 and 1693 cm^{-1}), alkenyl (1638 cm^{-1}), and aromatic (1607, 1518, and 1463 cm^{-1}) functionalities. The NMR data of **9** (Table 3) clearly showed signals for two carbonyl groups (δ_C 203.4 and 191.3), one 1,2,4-trisubstitute phenyl ring [δ_H 6.80 (d, $J = 8.2$ Hz), 6.62 (br d, $J = 8.2$ Hz), and 6.51 (br s)], one allyl group [δ_H 5.64 (m), 5.07 (d, $J = 10.0$ Hz), 5.04 (d, $J = 17.1$ Hz), 2.22 (dd, $J = 14.8$, 7.9 Hz), and 2.05 (dd, $J = 14.8$, 7.0 Hz)], one trisubstituted double bond [δ_H 6.28 (s)], three methoxy groups [δ_H 3.87 (3H,s), 3.86 (3H, s), and 3.70 (3H,s)], and one methyl group [δ_H 1.08 (3H, d, $J = 7.1$ Hz)]. By comparison of the NMR data of **9** with those of the known bicyclooctanoid [3.2.1] neolignans, denudadiones A–C (Kuroyanagi et al., 2000), compound **9** was determined to be a bicyclooctanoid neolignan. The ^{1}H–^{1}H COSY correlations of **9** (Fig. 3) showed the presence of two fragments C-7 to C-9 and C-7′ to C-9′. The overall structure of **9** was determined to be 5-allyl-6-(3,4-dimethoxyphenyl)-3-methoxy-7-methylbicyclo[3.2.1]oct-3-ene-2,8- dione by the key HMBC correlations (Fig. 3) from H-7 to C-2 and C-6, H-8 to C-2′ and C-4′, H-3′ to C-5′, 5′-OMe to C-5′, H-7′ to C-7, C-2′ and C-6′, and H-8′ to C-1′.

The relative configuration of **9** (piperbonin C) was confirmed by the key ROESY correlations (Fig. 3) of H-7/H_3-9 and H-7/H-6′. However, the absolute configuration of compound **9** remains undefined.

The known compounds (+)-*trans*-acuminatin (**10**) (El-Feraly et al., 1982; López-Sánchez et al., 2013), (+)-*cis*-acuminatin (**11**) (López-Sánchez et al., 2013), (+)-kadsurenone (**12**) (Chang et al., 1985), (+)-burchellin (**13**) (Lima et al., 1972; Li et al., 1987), (+)-kadsurenin M (**14**) (Nascimento and Lopes, 1999), (+)-virolin (**15**) (Barata et al., 1978; Zacchino and Badano, 1985), galgravin (**16**) (Birch et al., 1958; Zhao and Ruan, 2006), 5-hydroxy-4′,7-dimethoxyflavone (**17**) (Yu et al., 2005), pipernonaline (**18**) (Lee et al., 2001), (+)-3′,4′-dimethoxybmzoic acid-(3″4″-dimethoxyphenyl)-2-methyl-3-oxobutyl ester (**19**) (López et al., 1995; Li et al., 2013), and ferrudiol (**20**) (Kijjoa et al., 2002) were determined by comparing their NMR data (for all compounds) and optical rotation values (for the neolignans) with those reported in the literature.

The inhibitory activity of selected isolates (**1**–**18**) was evaluated against platelet aggregation induced by thrombin (Table 4). Piperbonin A (**7**), (+)-*trans*-acuminatin (**10**), (+)-*cis*-acuminatin (**11**), (+)-kadsurenone (**12**), and pipernonaline (**18**) showed weak activity with IC_{50} values of 118.2, 108.5, 90.02, 107.3, and 116.3 μM, respectively, as compared with the positive control, tirofiban, with an IC_{50} value of 5.24 μM. (+)-Kadsurenone is a noted platelet-activating factor (PAF) receptor antagonist from *P. kadsura* (Shen et al., 1985). It has previously been reported to inhibit the platelet release reaction induced by thrombin (Teng et al., 1991). The inhibitory activity of pipernonaline against thrombin-induced platelet aggregation has previously been tested (Park et al., 2007), whereas the activities of piperbonin A, (+)-*trans*-acuminatin, and (+)-*cis*-acuminatin have only been reported in the present study. Among the dihydrobenzofuran neolignans, (+)-*trans*-acuminatin and (+)-*cis*-acuminatin with a propenyl group at C-1′ were more potent than (+)-kadsurenin M with a formyl group at C-1′, i.e. in eliciting an inhibitory effect of thrombin-induced platelet aggregation.

Thrombin receptor antagonists are a novel class of antiplatelet agents that inhibit thrombin-mediated platelet activation. In May 2014, the US Food and Drug Administration (FDA) approved vorapaxar, a synthetic tricyclic 3-phenylpyridine analogue of the naturally occurring alkaloid himbacine, for the prevention of thrombotic cardiovascular events in patients with a history of myocardial infarction (MI) or peripheral arterial disease (PAD). Vorapaxar functions as a thrombin receptor antagonist, working against the protease activated receptor 1 (PAR1) to inhibit platelet aggregation without affecting hemostasis (Hashemzadeh et al., 2015). The inhibition of thrombin induced platelet aggregation implies that these active compounds from *P. bonii* may be inhibitors of PAR1 or PAR4.

Some *Piper* plants are traditionally used against cancer or cancer-like symptoms, and amides are the major active constituents (Wang et al., 2014b). Therefore, the new amides (**1**–**6**) from the plant were also evaluated for their growth inhibitory activities against HL-60 (human leukemia), A-549 (human lung cancer), MCF-7 (human breast cancer), SMMC-7721 (human liver cancer), and SW480 (human rectal cancer) cell lines with the positive control *cis*-platinum with IC_{50} values of 2.38, 12.10, 18.79, 9.67, and 8.77 μM, respectively. However, all of the tested compounds were inactive at concentrations up to 40 μM. Piperbonamides A–F (**1**–**6**) belong to arylalkenylacyl amides with a 2-(4-hydroxyphenyl)ethylamino moiety. Previous findings showed that the presence of a pyrrolidin-1-yl or piperidin-1-yl unit is important for the

Table 4
The effect of compounds on rabbit platelet aggregation induced by thrombin (2 U/mL)[a].

Compound	IC_{50} (μM)
Piperbonin A (**7**)	118.2
(+)-*trans*-Acuminatin (**10**)	108.5
(+)-*cis*-Acuminatin (**11**)	90.02
(+)-Kadsurenone (**12**)	107.3
Pipernonaline (**18**)	116.3
Tirofiban (positive control)	5.24

[a] The inhibition of other tested compounds (**1**–**6**, **8**, **9**, and **13**–**17**) was less than 30% at the concentration of 100 μM.

Please cite this article in press as: Ding, D.-D., et al., Amides and neolignans from the aerial parts of *Piper bonii*, Phytochemistry (2016), http://dx.doi.org/10.1016/j.phytochem.2016.07.004

cytotoxicity of arylalkenylacyl amides (Wang et al., 2014a). The present results further support this conclusion.

3. Conclusions

In the current study, six new amides (**1**–**6**), three new neolignans (**7**–**9**), and 11 known compounds (**10**–**20**) were obtained from the aerial parts of *Piper bonii* for the first time. Several compounds including four neolignans (**7**, **10**, **11**, and **12**) and one amide (**18**) showed weak activity against platelet aggregation induced by thrombin. Nevertheless, in future, it may be worth searching for new platelet antagonists from the *Piper* plants or the traditional Chinese medicines with the functions of "Huoxue" or "Huayu".

4. Experimental

4.1. General experimental procedures

Optical rotations were recorded using a JASCO P-1020 Polarimeter (Jasco Corp., Tokyo, Japan). UV spectra were taken on a Shimadzu UV-2401 PC spectrophotometer (Shimadzu, Kyoto, Japan). Electronic circular dichroism (ECD) spectra were recorded on a Chirascan CD spectrometer (Applied Photophysics Ltd., Leatherhead, UK). IR spectra were measured on a Bruker Tensor 27 FTIR Spectrometer (Bruker Corp., Ettlingen, Germany) with KBr disks. ^{1}H and ^{13}C NMR spectra were collected on a Bruker AM-400, DRX-500 and Avance III-600 spectrometers (Bruker Bio-Spin GmbH, Rheinstetten, Germany) with TMS as an internal standard. ESIMS and HRESIMS analyses were performed on an API QSTAR Pulsar 1 spectrometer (Applied Biosystems/MDS Sciex, Foster City, CA, USA). HREIMS were performed on a Waters AutoSpec Premier p776 spectrometer (Waters, Millford, MA, USA). Silica gel G (80—100 and 300—400 mesh, Qingdao Meigao Chemical Co., Ltd., Qingdao, China), C_{18} silica gel (40—75 μm, Fuji Silysia Chemical Ltd., Aichi, Japan), and Sephadex LH-20 (GE Healthcare Bio-Sciences AB, Uppsala, Sweden) were used for column chromatography (CC), and silica gel GF_{254} (Qingdao Meigao Chemical Co., Ltd.) was used for preparative TLC as precoated plates. TLC spots were visualized under UV light at 254 nm and by dipping into 5% H_2SO_4 in alcohol followed by heating. Semipreparative HPLC was performed on an Agilent 1200 series pump (Agilent Technologies, Santa Clara, USA) equipped with a diode array detector and a Waters XBridge C_{18} column (5.0 μm, ϕ 10 × 250 mm) and an Agilent Zorbax SB-C_{18} column (5.0 μm, ϕ 9.4 × 250 mm).

4.2. Plant material

Aerial parts of *P. bonii* were collected from Xishuangbanna of Yunnan Province, People's Republic of China, in June 2012. Based on the taxonomic system in *Flora of China*, the plant was identified by one of the authors (C.-L.L.), and a voucher specimen (No. 201201) was deposited at the Key Laboratory of Economic Plants and Biotechnology, Kunming Institute of Botany, Chinese Academy of Sciences.

4.3. Extraction and isolation

Air-dried, powdered aerial parts of *P. bonii* (2.5 kg) were exhaustively extracted with MeOH (4 × 10 L) at room temperature. The combined MeOH extract (430 g) was suspended in H_2O (2 L) and further partitioned with petroleum ether (3 × 2 L) and $CHCl_3$ (3 × 2 L), respectively. The petroleum ether-soluble part (A, 51.2 g) was subjected to silica gel CC (petroleum ether/EtOAc, 20:1 → 0:1, v/v) to yield six fractions (A1—A6). Fraction A2 was separated on an RP-18 silica gel column eluted with MeOH/H_2O (10% MeOH → 100%) to yield two main subfractions (A2-1 and A2-2). Subfraction A2-1 [the MeOH/H_2O (7030:) eluted portion] was purified by Sephadex LH-20 CC (MeOH), silica gel CC (petroleum ether/EtOAc, 15:1, v/v), and semipreparative HPLC (Waters XBridge C_{18} column, 10 × 250 mm, MeOH/H_2O, 752 ,25: mL/min) to give **11** (23.8 mg, t_R = 7.566 min) and **10** (4.5 mg, t_R = 8.162 min). Subfraction A2-2 [the MeOH/H_2O (8020:) eluted portion] was purified by Sephadex LH-20 CC (MeOH) and silica gel CC (petroleum ether/EtOAc, 15:1, v/v) to obtain **18** (32.7 mg). Fraction A3 was separated on an RP-18 silica gel column eluted with MeOH/H_2O (10% MeOH → 100%) to yield two main subfractions (A3-1 and A3-2). Subfraction A3-1 [the MeOH/H_2O (6040:) eluted portion] was purified by Sephadex LH-20 CC (MeOH), silica gel CC (petroleum ether/EtOAc, 15:1, v/v), and semipreparative HPLC (Waters XBridge C_{18} column, 10 × 250 mm, MeOH/H_2O, 752 ,25: mL/min) to yield **12** (334.2 mg, t_R = 14.189 min). Subfraction A3-2 [the MeOH/H_2O (7030:) eluted portion] was purified by Sephadex LH-20 CC (MeOH) and silica gel CC (petroleum ether/EtOAc, 15:1, v/v) to give **17** (4.5 mg). Fraction A4 was separated on an RP-18 silica gel column eluted with MeOH/H_2O (10% MeOH → 100%) to yield three main subfractions (A4-1 to A4-3). Subfraction A4-1 [the MeOH/H_2O (6040:) eluted portion] was purified by Sephadex LH-20 CC (MeOH), silica gel CC ($CHCl_3$/MeOH, 20:1, v/v), and semipreparative HPLC (Waters XBridge C_{18} column, 10 × 250 mm, MeOH/H_2O, 7030:, 2 mL/min) to give **8** (4.5 mg, t_R = 10.307 min) and **9** (6.2 mg, t_R = 12.918 min). Subfraction A4-2 [the MeOH/H_2O (7030:) eluted portion] was isolated by Sephadex LH-20 CC (MeOH), silica gel CC ($CHCl_3$/EtOAc, 20:1, v/v), and further purified by semipreparative HPLC (Agilent Zorbax SB-C_{18} column, 9.4 × 250 mm, 2 mL/min) to yield **14** (4.0 mg; MeOH/H_2O, 7030:; t_R = 8.845 min), **15** (4.8 mg; CH_3CN/H_2O, 6535:; t_R = 12.458 min), and **16** (4.1 mg; CH_3CN/H_2O, 6535:; t_R = 16.765 min). Subfraction A4-3 [the MeOH/H_2O (8020:) eluted portion] was purified by Sephadex LH-20 CC (MeOH) and silica gel CC (petroleum ether/acetone, 10:1, v/v) to give **7** (145.5 mg).

The $CHCl_3$-soluble part (B, 13.5 g) was subjected to silica gel CC using $CHCl_3$/MeOH (30:1 → 20:1, v/v) to afford a major fraction. This fraction was further separated on an RP-18 silica gel column eluted with MeOH/H_2O (10% MeOH → 100%) to yield three main subfractions (B1-1 to B1-3). Subfraction B1-1 [the MeOH/H_2O (6040:) eluted portion] was purified by Sephadex LH-20 CC (MeOH), silica gel CC ($CHCl_3$/MeOH, 20:1, v/v), and semipreparative HPLC (Agilent Zorbax SB-C_{18} column, 9.4 × 250 mm, CH_3CN/H_2O, 702 ,30: mL/min) to give **4** (5.1 mg, t_R = 15.900 min), **20** (3.0 mg, t_R = 16.893 min), **5** (4.9 mg, t_R = 24.073 min), and **6** (5.2 mg, t_R = 28.512 min). Subfraction B1-2 [the MeOH/H_2O (7030:) eluted portion] was purified by Sephadex LH-20 CC (MeOH), silica gel CC ($CHCl_3$/MeOH, 20:1, v/v), and semipreparative HPLC (Waters XBridge C_{18} column, 10 × 250 mm, MeOH/H_2O, 802 ,20: mL/min) to obtain **1** (5.2 mg, t_R = 18.372 min), **2** (3.5 mg, t_R = 21.206 min), and **3** (3.5 mg, t_R = 32.642 min). Subfraction B1-3 [the MeOH/H_2O (8020:) eluted portion] was purified by Sephadex LH-20 CC (MeOH), silica gel CC ($CHCl_3$/MeOH, 20:1, v/v), and semipreparative HPLC (Waters XBridge C_{18} column, 10 × 250 mm, MeOH/H_2O, 702 ,30: mL/min) to yield **19** (4.5 mg, t_R = 8.776 min) and **13** (5.0 mg, t_R = 24.290 min).

4.4. Piperbonamide A (*1*)

Pale green oil; UV (MeOH) λ_{max} (log ε) 261 (4.48), 226 (4.33) nm; IR (KBr) ν_{max} 3396, 2925, 2852, 1657, 1627, 1610, 1596, 1532, 1514, 1449, 1231, 999, 968, 829 cm^{-1}; For ^{1}H and ^{13}C NMR spectroscopic data, see Table 1; ESIMS *m*/*z* 442 $[M+Na]^+$; HRESIMS *m*/*z* 442.2352 $[M+Na]^+$ (calcd for $C_{27}H_{33}NNaO_3$, 442.2353).

Please cite this article in press as: Ding, D.-D., et al., Amides and neolignans from the aerial parts of *Piper bonii*, Phytochemistry (2016), http://dx.doi.org/10.1016/j.phytochem.2016.07.004

4.5. Piperbonamide B (**2**)

Pale green oil; UV (MeOH) λ_{max} (log ε) 273 (3.78), 222 (4.48) nm; IR (KBr) ν_{max} 3405, 2924, 2852, 1668, 1628, 1614, 1598, 1534, 1514, 1449, 1238, 969, 827 cm^{-1}; For ^1H and ^{13}C NMR spectroscopic data, see Table 1; ESIMS *m/z* 444 $[M+Na]^+$; HRESIMS *m/z* 444.2512 $[M+Na]^+$ (calcd for $C_{27}H_{35}NNaO_3$, 444.2509).

4.6. Piperbonamide C (**3**)

Pale green oil; UV (MeOH) λ_{max} (log ε) 261 (4.44), 226 (4.28) nm; IR (KBr) ν_{max} 3417, 2920, 2850, 1655, 1626, 1613, 1596, 1544, 1514, 1465, 1447, 1262, 1239, 1005, 830 cm^{-1}; For ^1H and ^{13}C NMR spectroscopic data, see Table 1; ESIMS *m/z* 470 $[M+Na]^+$, 917 $[2M+Na]^+$; HRESIMS *m/z* 470.2688 $[M+Na]^+$ (calcd for $C_{29}H_{37}NNaO_3$, 470.2666).

4.7. Piperbonamide D (**4**)

Pale green oil; UV (MeOH) λ_{max} (log ε) 300 (3.69), 263 (4.06) nm; IR (KBr) ν_{max} 3426, 2925, 2853, 1665, 1624, 1548, 1515, 1504, 1491, 1445, 1247, 1038 cm^{-1}; For ^1H and ^{13}C NMR spectroscopic data, see Table 2; ESIMS *m/z* 444 $[M+Na]^+$, 865 $[2M+Na]^+$; HRESIMS *m/z* 444.2144 $[M+Na]^+$ (calcd for $C_{26}H_{31}NNaO_4$, 444.2145).

4.8. Piperbonamide E (**5**)

Pale green oil; UV (MeOH) λ_{max} (log ε) 303 (3.71), 262 (4.57) nm; IR (KBr) ν_{max} 3427, 2924, 2852, 1655, 1629, 1614, 1546, 1515, 1504, 1445, 1247, 1038, 995 cm^{-1}; For ^1H and ^{13}C NMR spectroscopic data, see Table 2; ESIMS *m/z* 470 $[M+Na]^+$, 917 $[2M+Na]^+$; HRESIMS *m/z* 470.2304 $[M+Na]^+$ (calcd for $C_{28}H_{33}NNaO_4$, 470.2302).

4.9. Piperbonamide F (**6**)

Pale green oil; UV (MeOH) λ_{max} (log ε) 303 (3.59), 262 (4.02) nm; IR (KBr) ν_{max} 3443, 2925, 2852, 1664, 1625, 1549, 1516, 1504, 1490, 1446, 1248, 1039 cm^{-1}; For ^1H and ^{13}C NMR spectroscopic data, see Table 2; ESIMS *m/z* 472 $[M+Na]^+$, 921 $[2M+Na]^+$; HRESIMS *m/z* 472.2456 $[M+Na]^+$ (calcd for $C_{28}H_{35}NNaO_4$, 472.2458).

4.10. Piperbonin A (**7**)

Pale yellow oil; $[\alpha]^{23}_D$ +56 (*c* 0.7, MeOH); $[\alpha]^{25}_D$ +47 (*c* 1.0, $CHCl_3$); UV (MeOH) λ_{max} (log ε) 309 (3.95), 278 (4.13), 230 (4.32) nm; ECD $\Delta\varepsilon$ (*c* 0.10, MeOH) +0.90 (232), +1.42 (204); IR (KBr) ν_{max} 2936, 1737, 1630, 1604, 1596, 1512, 1465, 1453, 1419, 1374, 1264, 1238, 1140, 1029, 966 cm^{-1}; For ^1H and ^{13}C NMR spectroscopic data, see Table 3; ESIMS *m/z* 423 $[M+Na]^+$, HRESIMS *m/z* 423.1781 $[M+Na]^+$ (calcd for $C_{23}H_{28}NaO_6$, 423.1778).

4.11. Piperbonin B (**8**)

Pale yellow oil; $[\alpha]^{23}_D$ +72 (*c* 0.3, MeOH); UV (MeOH) λ_{max} (log ε) 309 (3.95), 278 (4.13), 230 (4.32) nm; ECD $\Delta\varepsilon$ (*c* 0.00672, MeOH) +0.27 (276), +0.67 (235), +2.10 (208); IR (KBr) ν_{max} 2937, 1739, 1684, 1593, 1508, 1465, 1423, 1375, 1268, 1138, 1029, 813 cm^{-1}; For ^1H and ^{13}C NMR spectroscopic data, see Table 3; ESIMS *m/z* 411 $[M+Na]^+$, HREIMS *m/z* 388.1522 $[M]^+$ (calcd for $C_{21}H_{24}O_7$, 388.1522).

4.12. Piperbonin C (**9**)

Pale yellow oil; $[\alpha]^{20}_D$ −70 (*c* 0.3, MeOH); UV (MeOH) λ_{max} (log ε) 280 (3.68), 228 (3.95) nm; ECD $\Delta\varepsilon$ (*c* 0.015, MeOH) −1.54 (330), +0.30 (302), −0.23 (293), +0.54 (277), −0.19 (259), +0.59 (218); IR (KBr) ν_{max} 2960, 2931, 1759, 1693, 1638, 1607, 1518, 1463, 1262, 1146, 1027 cm^{-1}; For ^1H and ^{13}C NMR spectroscopic data, see Table 3; ESIMS *m/z* 379 $[M+Na]^+$; HRESIMS *m/z* 379.1520 $[M+Na]^+$ (calcd for $C_{21}H_{24}NaO_5$, 379.1516).

4.13. In vitro platelet aggregation assay

New Zealand rabbits (male, 2.0–2.5 kg) were purchased from Nanjing Qinglongshan Animal Center (Nanjing, China). All animals were acclimated for at least 1 week at a temperature of 22 ± 2 °C and humidity of 55 ± 5% in a 12-h light-dark cycle with free access to food and H_2O. All protocols were approved by the Committee on the Ethics of Animal Experiments of China Pharmaceutical University and conformed to the National Institutes of Health Guideline for Care and Use of Laboratory Animals.

In vitro platelet aggregation was conducted using the turbidimetric method with a minor modification (Aghaloo et al., 2002; Nishikawa and Hidaka, 1982). Briefly, blood was withdrawn from the carotid artery of New Zealand rabbits after local anaesthesia with lidocaine, and collected into tubes containing 3.8% sodium citrate (1:9 citrate/blood, v/v) and centrifuged for 15 min at 950 rpm to prepare platelet-rich plasma (PRP) or 10 min at 3000 rpm to obtain platelet-poor plasma (PPP), respectively. The platelet concentration was adjusted to 3×10^8 platelets/mL with PPP. A 270 μL aliquot of PRP was preincubated at 37 °C for 5 min in the cuvette with 20 μL of the sample or vehicle (saline), and then platelet aggregation was induced by addition of 10 μL thrombin (2 U/mL, Sigma Chemical Co., St. Louis, MO, USA). The maximum platelet aggregation rate was defined as the maximal percentage increase in light transmission after addition of thrombin related to the light transmission in PPP, and the maximum aggregation rate was determined within 5 min with continuous stirring at 37 °C using a four-channel aggregometer (Beijing Steellex Science Instrument Company, China). The IC_{50} values were defined as the concentration of inhibitor that cause a 50% inhibition to the platelet aggregation, and was calculated using GraphPad Prism 6 (GraphPad Software, Inc., La Jolla, CA, USA).

4.14. MTS assay for cytotoxicity

The isolated amides were tested *in vitro* for their cytotoxicity against proliferation of human leukemia HL-60, human lung cancer A-549, human breast cancer MCF-7, human liver cancer SMMC-7721, and human rectal cancer SW480 cell lines using the MTS assay (Mosmann, 1983). The 3-(4,5-dimethylthiazol-2-yl)-5(3-carboxymethoxyphenyl)-2-(4-sulfopheny)-2*H*-tetrazolium (MTS) (Promega, Beijing, China) mix-based cell titer assays were performed as previously described. In general, cells in log-phase of their cycle were seeded in 96-well plates (5000–10,000 cells/well, NEST Biotechnology, Wuxi, China) in a 100 μL volume, with paired single cell suspension containing 10% fetal bovine serum (DMEM or RMPI1640, Thermo Fisher Scientific, Beijing, China). These were then treated with indicated concentrations of the compounds dissolved in DMSO, which were set the regular thickness of 40 μM for the initial screening and five concentrations of each compound were fixed in the concentration compounds inhibition tumor cell growth about 50% to achieve a total culture medium in a volume of 200 μL. After incubation for 48 h at 37 °C, an MTS (20 μL) solution and DMEM (100 μL) were added into the well, incubation was continued for another 1–4 h. The absorbance was measured at the detection wavelength of 490 nm (L_1) and the reference wavelength of 680 nm (L_2) and cytotoxicity was expressed as IC_{50} values (Reed and Muench, 1938). *Cis*-platinum (Sigma) was used as the positive control.

Please cite this article in press as: Ding, D.-D., et al., Amides and neolignans from the aerial parts of *Piper bonii*, Phytochemistry (2016), http://dx.doi.org/10.1016/j.phytochem.2016.07.004

Acknowledgments

We gratefully acknowledge Dr. Kendrick Marr from the Royal British Columbia Museum for proofreading this manuscript. This work was funded by the Ministry of Science & Technology of China (2012FY110300), the National Natural Science Foundation of China (3116140345), the Minzu University of China (YLDX01013, 2015MDTD16C), and the Natural Science Foundation of Yunnan Province, China (2011FZ205).

Appendix A. Supplementary data

Supplementary data related to this article can be found at http://dx.doi.org/10.1016/j.phytochem.2016.07.004.

References

Aghaloo, T.L., Moy, P.K., Freymiller, E.G., 2002. Investigation of platelet-rich plasma in rabbit cranial defects: a pilot study. J. Oral Maxil. Surg. 60, 1176–1181.

Braga, A.C.H., Zacchino, S., Badano, H., Sierra, M.G., Rúveda, E.A., 1984. ^{13}C NMR spectral and conformational analysis of 8-*O*-4′ neolignans. Phytochemistry 23, 2025–2028.

Barata, L.E., Baker, P.M., Gottlieb, O.R., Rùveda, E.A., 1978. Neolignans of *Virola surinamensis*. Phytochemistry 17, 783–786.

Birch, A., Milligan, B., Smith, E., Speake, R., 1958. Some stereochemical studies of lignans. J. Chem. Soc. 4471–4476.

Cao, G.-Y., Xu, W., Yang, X.-W., Gonzalez, F.J., Li, F., 2015. New neolignans from the seeds of *Myristica fragrans* that inhibit nitric oxide production. Food Chem. 173, 231–237.

Chang, M.N., Han, G.-Q., Arison, B.H., Springer, J.P., Hwang, S.-B., Shen, T.Y., 1985. Neolignans from *Piper futokadsura*. Phytochemistry 24, 2079–2082.

Chen, C., Yang, F.-Q., Zhang, Q., Wang, F.-Q., Hu, Y.-J., Xia, Z.-N., 2015. Natural products for antithrombosis. Evid.-Based Compl. Alt. Med. 2015. Article ID 876426, http://www.hindawi.com/journals/ecam/2015/876426/.

Chen, S., Cheng, M.-J., Wu, C.-C., Peng, C.-F., Huang, H.-Y., Chang, H.-S., Wang, C.-J., Chen, I.-S., 2014. Three new phenylpropanoids from the roots of *Piper taiwanense* and their inhibitory activities on platelet aggregation and *Mycobacterium tuberculosis*. Chem. Biodivers. 11, 792–799.

Chen, S., Huang, H.-Y., Cheng, M.-J., Wu, C.-C., Ishikawa, T., Peng, C.-F., Chang, H.-S., Wang, C.-J., Wong, S.-L., Chen, I.-S., 2013. Neolignans and phenylpropanoids from the roots of *Piper taiwanense* and their antiplatelet and antitubercular activities. Phytochemistry 93, 203–209.

Chen, Y.-C., Liao, C.-H., Chen, I.-S., 2007. Lignans, an amide and anti-platelet activities from *Piper philippinum*. Phytochemistry 68, 2101–2111.

Curti, C., Zanardi, F., Battistini, L., Sartori, A., Rassu, G., Pinna, L., Casiraghi, G., 2006. Streamlined, asymmetric synthesis of 8,4'-oxyneolignans. J. Org. Chem. 71, 8552–8558.

Editorial Board of "Zhonghua Bencao", 1999. Zhonghua Bencao, vol. 3. Shanghai Scientific and Technological Press, Shanghai, pp. 424–449.

El-Feraly, F.S., Cheatham, S.F., Hufford, C.D., Li, W.-S., 1982. Optical resolution of (±)-dehydrodiisoeugenol: structure revision of acuminatin. Phytochemistry 21, 1133–1135.

Fontenele, J.B., Leal, L., Silveira, E.R., Felix, F.H., Felipe, C.F.B., Viana, G.S., 2009. Antiplatelet effects of piplartine, an alkamide isolated from *Piper tuberculatum*: possible involvement of cyclooxygenase blockade and antioxidant activity. J. Pharm. Pharmacol. 61, 511–515.

Hao, H.-Z., He, A.-D., Wang, D.-C., Yin, Z., Zhou, Y.-J., Liu, G., Liang, M.-L., Da, X.-W., Yao, G.-Q., Xie, W., Xiang, J.-Z., Ming, Z.-Y., 2015. Antiplatelet activity of loureirin A by attenuating Akt phosphorylation: *in vitro* studies. Eur. J. Pharmacol. 746, 63–69.

Hashemzadeh, M., Movahed, M.R., Arreguin, J.M., 2015. Vorapaxar: a new antiplatelet therapy. Cardiol. Pharmacol. 4, 128.

Hu, L., Chen, Z., Xie, Y., Jiang, Y., Zhen, H., 2000. Alkyl and alkoxycarbonyl derivatives of ginkgolide B: synthesis and biological evaluation of PAF inhibitory activity. Bioorgan. Med. Chem. 8, 1515–1521.

Huang, Z.S., Zeng, C.L., Zhu, L.J., Jiang, L., Li, N., Hu, H., 2010. Salvianolic acid A inhibits platelet activation and arterial thrombosis via inhibition of phosphoinositide 3-kinase. J. Thromb. Haemost. 8, 1383–1393.

Iwashita, M., Oka, N., Ohkubo, S., Saito, M., Nakahata, N., 2007. Piperlongumine, a constituent of *Piper longum* L., inhibits rabbit platelet aggregation as a thromboxane A 2 receptor antagonist. Eur. J. Pharmacol. 570, 38–42.

Kato, M.J., Furlan, M., 2007. Chemistry and evolution of the Piperaceae. Pure Appl. Chem. 79, 529–538.

Kijjoa, A., Bessa, J., Pinto, M.M., Anatachoke, C., Silva, A.M., Eaton, G., Herz, W., 2002. Polyoxygenated cyclohexene derivatives from *Ellipeiopsis cherrevensis*. Phytochemistry 59, 543–549.

Kuroyanagi, M., Yoshida, K., Yamamoto, A., Miwa, M., 2000. Bicyclo[3.2.1]octane and 6-oxabicyclo[3.2.2]nonane type neolignans from *Magnolia denudata*. Chem. Pharm. Bull. 48, 832–837.

López-Sánchez, C., Álvarez-Corral, M., Jiménez-González, L., Muñoz-Dorado, M., Rodríguez-García, I., 2013. Rh (II)-catalyzed enantioselective synthesis of acuminatin through a C–H insertion reaction of a non-stabilized carbenoid. Tetrahedron 69, 5511–5516.

López, H., Valera, A., Trujillo, J., 1995. Lignans from *Ocotea foetens*. J. Nat. Prod. 58, 782–785.

Lee, S.-E., Park, B.-S., Kim, M.-K., Choi, W.-S., Kim, H.-T., Cho, K.-Y., Lee, S.-G., Lee, H.-S., 2001. Fungicidal activity of pipernonaline, a piperidine alkaloid derived from long pepper, *Piper longum* L., against phytopathogenic fungi. Crop Prot. 20, 523–528.

Li, C.-Y., Tsai, W.-J., Damu, A.G., Lee, E.-J., Wu, T.-S., Dung, N.X., Thang, T.D., Thanh, L., 2007. Isolation and identification of antiplatelet aggregatory principles from the leaves of *Piper lolot*. J. Agric. Food. Chem. 55, 9436–9442.

Li, S.-M., Han, G.-Q., Arison, B.H., Chang, M.N., 1987. Studies on chemical constituents of *Piper hancei* Maxim (II). Acta Pharm. Sin. 22, 196–202.

Li, Y.-F., Jiang, Y., Huang, J.-F., Yang, G.-Z., 2013. Four new lignans from *Schisandra sphenanthera*. J. Asian Nat. Prod. Res. 15, 934–940.

Lima, O.A., Gottlieb, O., Magalhães, M.T., 1972. Burchellin, a neolignan from *Aniba burchellii*. Phytochemistry 11, 2031–2037.

Lin, L.-C., Tsai, T.-H., Su, S.-C., 2011. A novel 8.*O*.6′-neolignan from *Taxillus theifer*. Nat. Prod. Res. 25, 1319–1323.

Liu, H.-X., He, M.-T., Tan, H.-B., Gu, W., Yang, S.-X., Wang, Y.-H., Li, L., Long, C.-L., 2015. Xanthine oxidase inhibitors isolated from *Piper nudibaccatum*. Phytochem. Lett. 12, 133–137.

Liu, L., Li, J., Zhang, Y., Zhang, S., Ye, J., Wen, Z., Ding, J., Kunapuli, S.P., Luo, X., Ding, Z., 2014. Salvianolic acid B inhibits platelets as a P2Y(12) antagonist and PDE inhibitor: evidence from clinic to laboratory. Thromb. Res. 134, 866–876.

Liu, Y., Yin, H.-J., Shi, D.-Z., Chen, K.-J., 2012. Chinese herb and formulas for promoting blood circulation and removing blood stasis and antiplatelet therapies. Evid.-Based Compl. Alt. Med. 2012. Article ID 184503, http://www.hindawi.com/journals/ecam/2012/184503/abs/.

Mosmann, T., 1983. Rapid colorimetric assay for cellular growth and survival: application to proliferation and cyto-toxicity assays. J. Immunol. Methods 65, 55–63.

Nascimento, I.R., Lopes, L.M., 1999. 2,3-Dihydrobenzofuran neolignans from *Aristolochia pubescens*. Phytochemistry 52, 345–350.

Nishikawa, M., Hidaka, H., 1982. Role of calmodulin in platelet aggregation. Structure-activity relationship of calmodulin antagonists. J. Clin. Invest 69, 1348–1355.

Park, B.-S., Son, D.-J., Park, Y.-H., Kim, T., Lee, S.-E., 2007. Antiplatelet effects of acidamides isolated from the fruits of *Piper longum* L. Phytomedicine 14, 853–855.

Parmar, V.S., Jain, S.C., Bisht, K.S., Jain, R., Taneja, P., Jha, A., Tyagi, O.D., Prasad, A.K., Wengel, J., Olsen, C.E., 1997. Phytochemistry of the genus *Piper*. Phytochemistry 46, 597–673.

Reed, L.J., Muench, H., 1938. A simple method of estimating fifty per cent endpoints. Am. J. Hyg. 27, 493–497.

Santos, B.V.O., Chaves, E.V.L., Gray, A.I., 1998. Phenylalkanoids from *Piper marginatum*. Phytochemistry 49, 1381–1384.

Scott, I.M., Jensen, H.R., Philogene, B.J.R., Arnason, J.T., 2008. A review of *Piper* spp. (Piperaceae) phytochemistry, insecticidal activity and mode of action. Phytochem. Rev. 7, 65–75.

Shen, T., Hwang, S.-B., Chang, M.N., Doebber, T.W., Lam, M., Wu, M.S., Wang, X., Han, G.Q., Li, R.Z., 1985. Characterization of a platelet-activating factor receptor antagonist isolated from haifenteng (*Piper futokadsura*): specific inhibition of *in vitro* and *in vivo* platelet-activating factor-induced effects. Proc. Natl. Acad. Sci. U. S. A. 82, 672–676.

Sheu, J.-R., Kan, Y.-C., Hung, W.-C., Ko, W.-C., Yen, M.-H., 1997. Mechanisms involved in the antiplatelet activity of tetramethylpyrazine in human platelets. Thromb. Res. 88, 259–270.

Shi, Y.-N., Shi, Y.-M., Yang, L., Li, X.-C., Zhao, J.-H., Qu, Y., Zhu, H.-T., Wang, D., Cheng, R.-R., Yang, C.-R., Xu, M., Zhang, Y.-J., 2015. Lignans and aromatic glycosides from *Piper wallichii* and their antithrombotic activities. J. Ethnopharmacol. 162, 87–96.

Tang, G.-H., Chen, D.-M., Qiu, B.-Y., Sheng, L., Wang, Y.-H., Hu, G.-W., Zhao, F.-W., Ma, L.-J., Wang, H.-A., Huang, Q.-Q., Xu, J.-J., Long, C.-L., Li, J., 2011. Cytotoxic amide alkaloids from *Piper boehmeriaefolium*. J. Nat. Prod. 74, 45–49.

Teng, C.-M., Yu, S.-M., Ko, F.-N., Chen, C.-C., Wang, W.-C., Chen, K.-Y., Huang, Y.-L., Huang, T.-F., 1991. Comparison of the actions of some platelet-activating factor antagonists on platelets and aortic smooth muscles. Eur. J. Pharmacol. 205, 151–156.

Tseng, Y.C., Xia, N.H., Gilbert, M.G., 1999. Piperaceae. In: Wu, Z.Y., Raven, P.H., Hong, D.Y. (Eds.), Flora of China, vol. 4. Science Press/Missouri Botanical Garden Press, Beijing/St. Louis, pp. 110–129.

Wang, P., Luo, C.-H., Wang, Q.-X., Li, Q.-Y., Li, P., Yuan, X.-H., 2013. Antithrombotic effect of ligustrazine hydrochloride injection on the model of induced arteriovenous shunt thrombosis. J. Res. Med. Sci. 18, 704–706.

Wang, Y.-H., Goto, M., Wang, L.-T., Hsieh, K.-Y., Morris-Natschke, S.L., Tang, G.-H., Long, C.-L., Lee, K.-H., 2014a. Multidrug resistance-selective antiproliferative activity of *Piper* amide alkaloids and synthetic analogues. Bioorg. Med. Chem. Lett. 24, 4818–4821.

Wang, Y.-H., Morris-Natschke, S.L., Yang, J., Niu, H.-M., Long, C.-L., Lee, K.-H., 2014b. Anticancer principles from medicinal *Piper* plants. J. Tradit. Complement. Med. 4, 8–16.

Xin, N., Li, Y.-J., Li, Y., Dai, R.-J., Meng, W.-W., Chen, Y., Schlappi, M., Deng, Y.-L., 2011. Dragon's Blood extract has antithrombotic properties, affecting platelet

aggregation functions and anticoagulation activities. J. Ethnopharmacol. 135, 510–514.
Yang, J., Su, Y., Luo, J.-F., Gu, W., Niu, H.-M., Li, Y., Wang, Y.-H., Long, C.-L., 2013a. New amide alkaloids from *Piper longum* fruits. Nat. Prod. Bioprospect 3, 277–281.
Yang, S.-X., Sun, Q.-Y., Yang, F.-M., Hu, G.-W., Luo, J.-F., Wang, Y.-H., Long, C.-L., 2013b. Sarmentosumols A to F, new mono-and dimeric alkenylphenols from *Piper sarmentosum*. Planta Med. 79, 693–696.
Yu, Z.-W., Zhu, H.-Y., Yang, X.-S., Sun, Q.-Y., Hao, X.-J., 2005. Study on chemical constituents from *Incarvillea arguta* and their accelerating PC-12 cell differentiation. China J. Chin. Mat. Med. 30, 1335–1338.
Zacchino, S.A., Badano, H., 1985. Stereoselective synthesis of 8.O.4' neolignans: (±)-surinamensin and (±)-virolin. J. Nat. Prod. 48, 830–832.
Zhang, Y., Ma, X.-j., Shi, D.-z, 2015. Antiplatelet effect of active components derived from Chinese herbal medicine. Chin. J. Integr. Med. http://dx.doi.org/10.1007/s11655-11015-12297-11659.
Zhao, Y., Ruan, J.-L., 2006. Chemical constituents from *Piper wallichii*. J. Chin. Pharm. Sci. 15, 21–23.

Please cite this article in press as: Ding, D.-D., et al., Amides and neolignans from the aerial parts of *Piper bonii*, Phytochemistry (2016), http://dx.doi.org/10.1016/j.phytochem.2016.07.004